

Integration of carbon dioxide capture in a wine effluent biorefinery through the use of deep eutectic solvents

Carlos E. Guzmán Martínez^a, Valeria Caltzontzin Rabell^a, Sergio I. Martínez Guido^a, Salvador Hernández^b and Claudia Gutiérrez Antonio^{a*}

^a Universidad Autónoma de Querétaro, Facultad de Ingeniería, Querétaro, Querétaro, Mexico

^b Universidad de Guanajuato, Departamento de Ingeniería Química, Guanajuato, Guanajuato, Mexico

* Corresponding Author: claudia.gutierrez@uaq.mx

ABSTRACT

The wine industry generates large volumes of organic effluents, whose inadequate management poses significant environmental challenges but also offers opportunities for resource recovery. In this work, an integrated biorefinery scheme for the valorization of winery effluents is proposed and evaluated through steady-state simulation in Aspen Plus®. The biorefinery converts winery wastewater into a portfolio of value-added chemicals and biofuels, including levulinic acid, propylene glycol, formic acid, light gases, naphtha, sustainable aviation fuel, green diesel, and bioethanol, while enabling water recovery and carbon dioxide management. Two alternative CO₂ capture routes are analyzed and compared: a conventional CaO-based carbonation–calcination process and an innovative absorption system using deep eutectic solvents (DES), specifically choline chloride–urea. Technical performance is assessed through chemical oxygen demand (COD) removal, recovery, conversion, yield, and product mass ratios. Economic feasibility is evaluated using profit-based indicators, while environmental performance is quantified through CO₂-equivalent emissions associated with utility consumption. Results show that the proposed biorefinery achieves a COD removal efficiency of 99.99%, producing treated water compliant with Mexican regulations for internal reuse. The DES-based configuration reduces raw material costs by 48.86%, enables hydrogen recovery as an additional valuable product, and increases overall profit by 2.86% compared to the CaO-based scheme. Although the relative reduction in total CO₂ emissions is modest (≈0.5%), the DES configuration achieves an absolute annual reduction of 2, 198 t CO₂. Overall, the results demonstrate that integrating DES-based CO₂ capture into winery effluent biorefineries enhances economic performance and supports circular economy principles through waste valorization, water reuse, and emissions mitigation.

Keywords: Deep Eutectic Solvents, biorefinery, wine effluents, techno-economic analysis

INTRODUCTION

The wine industry plays an essential role in the global economy, with sales ranging between €25.8 and €31.4 billion [1]. Mexico, ranked 32nd among the world's wine producers, contributed approximately 400, 000 hectoliters in 2022 [2]. Moreover, the wine industry stands out due to the considerable volumes of organic effluents generated during pretreatment, fermentation, clarification, and bottling operations. On average, 2–4 liters of effluent are generated per liter of wine produced, underscoring the need for sustainable management

strategies. In this context, waste valorization offers a significant opportunity [3].

The wine effluents contain high concentrations of carbohydrates, alcohols, and organic matter. Because of their rich organic and mineral content, winery effluents are often reused for irrigation or discharged into water bodies and surrounding environments. However, if not properly treated, their high organic load and seasonal variability pose serious environmental risks. The impacts extend beyond aquatic systems to terrestrial ones. On land, effluents can cause salinization, acidification, structural soil damage, and unpleasant odors, while reducing

mineral availability, microbial diversity, and biological productivity. In aquatic systems, they can lead to turbidity, eutrophication, oxygen depletion, decreased photosynthesis, and toxic effects on aquatic life [3]. Nonetheless, their organic content also makes these effluents a promising feedstock for biorefinery systems. Due to this, several strategies have been analyzed to treat and valorize effluents derived from the wine industry. Among the analyzed processes, the valorization of wine effluents through biorefinery schemes is highlighted.

A biorefinery integrates a set of processes designed to convert wine effluents into value-added products, chemicals, biofuels, and bioenergy. In this processing scheme, the inclusion of carbon capture technologies aligns with circular-economy principles, promoting closed-loop systems that minimize waste and emissions. Among the available CO₂-capture approaches, absorption with chemical solvents is one of the most efficient and technologically mature. However, conventional amine-based solvents such as monoethanolamine (MEA) have significant drawbacks, including high regeneration energy requirements, solvent degradation, and environmental toxicity. As an alternative, deep eutectic solvents (DES) have emerged as a new generation of environmentally friendly solvents with outstanding physicochemical properties.

Various DES formulations have been explored, such as choline chloride/ethanolamine, choline chloride/L-arginine/glycerol, and choline chloride/1, 2-propanediol. Notably, the combination of choline chloride and urea forms a liquid solvent known as choline chloride:urea (ChCl:U) or reline, which demonstrates a high capacity for selectively absorbing CO₂ from gas mixtures [4].

Therefore, the research aim is to design and evaluate a conceptual process that integrates deep eutectic solvents-based CO₂ absorption with a biorefinery scheme. This scheme treats winery effluents to produce levulinic acid, sustainable aviation fuel (SAF), naphtha, light gas, formic acid, green diesel, propylene glycol, di-propylene glycol, and bioethanol. Additionally, in this biorefinery, water can be recovered to quality levels permissible under Mexican regulations.

METHODOLOGY

In general, the procedure implemented to develop the proposed biorefinery is summarized in the block flowchart shown in Figure 1.

First, the case study is defined in terms of the effluent composition and its mass flow rate. Subsequently, the target products are established, together with the unit operations required for their recovery and/or production; this stage corresponds to the conceptual process design.

To satisfy the CO₂ capture requirement within the

proposed biorefinery, two alternative capture routes are developed. The first route integrates CO₂ capture using deep eutectic solvents (DESs), whereas the second route is based on CaO as the capturing agent. Each route is incorporated into the overall process flowsheet to meet the CO₂ capture demand of the system. Consequently, these alternatives define two different biorefinery schemes, each one characterized by its corresponding CO₂ capture technology.

The kinetic and thermodynamic information reported in the literature is compiled and used to support the process modeling. Afterwards, the manipulated variables for each unit operation are identified, and the complete biorefinery is modeled and simulated under steady-state conditions using Aspen Plus® V15. Finally, technical, economic, and environmental assessments are carried out to evaluate the overall performance of the proposed biorefinery.

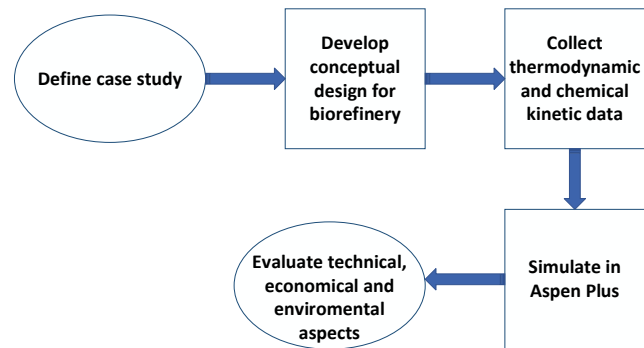


Figure 1. Methodological strategy

The technical evaluation aims to quantify the capacity of the biorefinery to remove contaminants from the effluent. This assessment is performed using the Chemical Oxygen Demand (COD) as a key indicator, calculated directly in Aspen Plus. Specifically, the technical performance is quantified through the relative reduction between the initial COD of the wine effluent and the COD of the treated water. In addition, several technical indicators are computed to characterize the overall process performance, namely: component recovery (*rec*), conversion (*cv*), yield (*Yd*), and product mass ratio (*pmr*), as defined by Equations (1)–(4) [5].

$$rec = \frac{oms}{fms} \quad (1)$$

$$cv = \frac{\dot{r}_{in} - \dot{r}_{out}}{\dot{r}_{in}} \quad (2)$$

$$yd = \frac{pmf}{tpm} \quad (3)$$

$$pmr = \frac{mp}{rmm} \quad (4)$$

Where: rec = component recuperation, oms = output mass flow (kg/h), fms = feed mass flow (kg/h) cv = conversion, r_{in} = reactant input to process (mol/h), r_{out} = reactant output to process (mol/h), Yd = Yield, pmf = moles of desired product formed (mol), tpm = theoretical product moles (mol), pmr = product mass ratio, mp = product mass flow (kg/h), rmm = raw material mass flow (kg/h)

The economic evaluation is based on the estimation of the process profit (PFT), defined as the difference between incomes and outcomes. Incomes correspond to product sales, whereas outcomes include raw material costs, total utility costs, and equipment-related costs. Equipment costs are estimated using the Guthrie method [6]. Since equipment investment represents a time-independent cost, an annualization factor (k) is incorporated to express this contribution on an annual basis [6]. The mathematical framework for the economic assessment is described by Equations (5)–(12). The parameters required to solve Equations (5)–(12), including Guthrie constants, are taken from Tourton et al. [6]. Utility prices were obtained from the Aspen Plus® V15 database. It is important to note that Guthrie parameters were originally developed in 2001; therefore, equipment costs were updated to 2025 values using the Marshall and Swift index and Equation (10) [6].

Finally, the environmental evaluation focuses on the environmental burden associated with utility consumption. The main indicator employed is the total CO₂-equivalent emissions, defined by Equation (13) and based on US-EPA-RULE-E9-5711. This parameter is also calculated using Aspen Plus.

$$PFT = (Ah)(P_{sale} - RMC - UC_T) - (k)(EC) \quad (5)$$

$$P_{sale} = \sum_1^j ((mp_j)(pp_j)) \quad (6)$$

$$RMC = \sum_1^g ((mp_g)(pp_g)) \quad (7)$$

$$UC_T = \sum_1^i (UC_i) \quad (8)$$

$$k = \frac{y(1+y)^h}{(1+y)^h - 1} \quad (9)$$

$$EC = C_2 = C_1 \left(\frac{I_2}{I_1} \right) \quad (10)$$

$$C_{BM} = C_p^o (B_1 + B_2 F_M F_P) \quad (11)$$

$$\log_{10} C_p^o = (K_1 + K_2 \log_{10}(A) + K_3 (\log_{10}(A))^2) \quad (12)$$

$$TCO_{2e} = \sum_1^l (CO_{2e_i}) \quad (13)$$

Where: PFT = profit (USD/year), Ah = hours per year (8766 h/year), PSALE = Product sales (USD/h), RMC = Raw material cost (USD/h), UCT = Total utilities cost (USD/h), k = annualization factor, EC = Equipment cost (USD), mp = product mass flow (kg/h), rmm = raw material mass flow (kg/h), pp = product price (USD/kg), prmm = raw material mass price (USD/kg), UC = Utility cost, y = interest rate (10 %), h = Life period of each technology (20 years), C_p^o = purchased cost for condition (USD), A = the capacity or size parameter for the equipment, (K₁, K₂, K₃, B₁, B₂) = Guthrie constants, FM = Material factor, FP = Pressure factor, CBM = bare module cost (USD), C₁ = Purchased cost to base time (USD), C₂ = Purchased cost to time when cost is desired (USD), I₁ = Cost index to base time, I₂ = Cost index to time when cost is desired, TCO_{2e} = Total CO₂ equivalent (ton CO₂ equivalent/year), CO_{2e_i} = CO₂ equivalent per utility (ton CO₂ equivalent/year). Subscripts: j = product stream, g = raw material stream, i = utility.

RESULTS

As previously mentioned, Mexico reported a wine production of 400, 000 hectoliters in 2022 [2]. According to Buitrón et al. [3], the wine industry generates between 0.2 and 4 L of wastewater per liter of wine produced. For the definition of the study case, the average value within this range was adopted, resulting in 2.1 L of wastewater per liter of wine. Therefore, the annual volume of wine effluent released in Mexico was estimated at 8.4×10^7 L·year⁻¹, which corresponds to 9, 589.04 L·h⁻¹. For modeling purposes, this value was rounded and, assuming the effluent density is close to that of water (as water is the predominant component), the study case was defined as a mass flow rate of 10, 000 kg·h⁻¹.

According to Buitrón et al. [3] winery effluent is composed of several components; however, the most abundant are water, solids, ethanol, and glucose. On the other hand, De Iseppi et al. [7] report that the solid fraction is constituted by 25 wt% lees, 25 wt% lignin, 25 wt% cellulose, and 25 wt% hemicellulose, mainly. It is important to mention that wine lees are dead yeast that are deposited and discarded at the clarification step of wine production. Table 1 shows the effluent characterization.

Regarding the thermodynamic model, it is not possible to use only one for the entire biorefinery; this is because the process uses several components, which have different characteristics such as organic or inorganic nature, in different amounts; therefore, thermodynamics models for each section are defined by Carlson algorithm [8]. Those used in the entire process are NRTL, BK10, and PENG-ROBINSON.

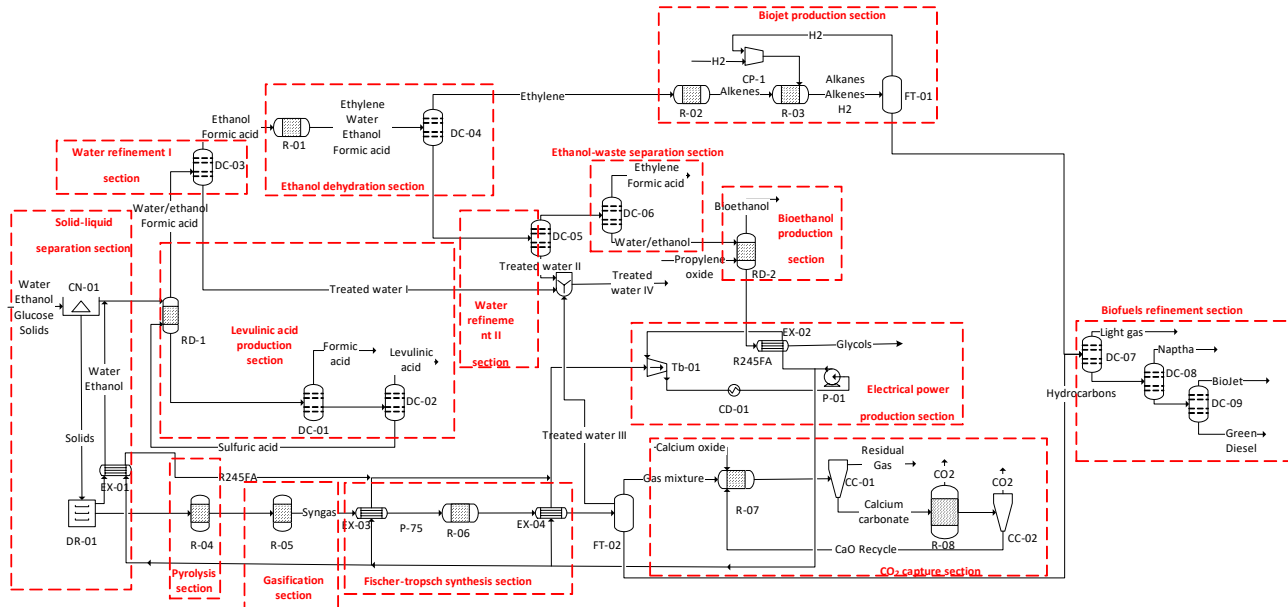


Figure 2. Biorefinery process flowsheet for the CaO-based CO₂ capture configuration.

Table 1: Winery effluent characterization

Winery effluent	Value
Mass flow (kg/h)	10,000
Water (wt%)	71.76
Ethanol (wt%)	7.39
Glucose (wt%)	5.26
Solids (wt%)	15.59
DQO (PPM)	210,052

The overall biorefinery scheme is presented in Figure 2. For clarity, the flowsheet is divided into several process sections. Figure 2 represents both the CaO-based and DES-based configurations; however, the only difference between them lies in the CO₂ capture section. For the DES configuration, the corresponding CO₂ capture section is shown separately in Figure 3, where CO₂ is captured using DESs [9].

The biorefinery process (Figure 2) begins with the separation of suspended solids from the bulk effluent. This step is performed using a centrifuge, and the recovered solids are routed to an independent processing pathway. The clarified liquid stream, mainly composed of glucose, ethanol, and water, is subsequently fed to a reactive distillation column (RD-01). In this unit, glucose is first converted to 5-hydroxymethylfurfural (5-HMF) and then further transformed into levulinic acid and formic acid. These reactions correspond to R1 and R2, respectively, while the kinetic parameters employed in the model are summarized in Table 2. The reaction system is catalyzed by H₂SO₄. Finally, the resulting acid mixture is purified using two conventional distillation columns (DC-01 and DC-02), enabling catalyst recovery and recycling.

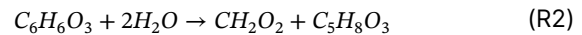
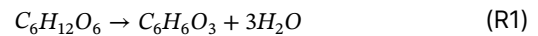


Table 2: Kinetic parameters for levulinic acid production [10]

Reaction	Reaction R1	Reaction R2
Preexponential factor (s ⁻¹)	2.09x10 ⁷	27,261.3
Activation energy (kJ/mol)	86.33	56.95

An overhead stream containing water, ethanol, and formic acid is withdrawn from RD-01. This stream is then fed to a third distillation column (DC-03), where ethanol and formic acid are recovered as the distillate, while treated water is obtained as the bottom product. The ethanol-rich stream is subsequently sent to reactor R-01, where ethanol is dehydrated to produce ethylene and water.

The ethylene produced in R-01 is purified in distillation column DC-04. The overhead stream, rich in ethylene, is sent to reactor R-02, where the polymerization step is carried out. The bottom stream from DC-04, containing heavier compounds and impurities, is directed to DC-05 for further treatment.

In R-02, the reaction yields a hydrocarbon mixture mainly composed of alkanes. This stream is subsequently hydrogenated to ensure full saturation of the products. Unreacted hydrogen is recovered in a flash tank (FT-01) and recycled, while the resulting hydrocarbon stream is

routed to the biofuels upgrading section.

Regarding the waste stream from DC-04, the water content is separated as the bottom product of DC-05, generating a second treated-water stream. The distillate from DC-05 is further processed in DC-06. In this column, ethylene and formic acid are recovered as the overhead product, whereas an ethanol-water mixture is obtained as the bottom stream.

The ethanol-water mixture is subsequently used as feedstock for bioethanol production. Ethanol dehydration is performed in a reactive distillation unit, where water reacts with propylene oxide to form propylene glycol. In addition, a side reaction between propylene oxide and propylene glycol leads to the formation of dipropylene glycol. These reactions correspond to R3 and R4, respectively, and the kinetic parameters employed are summarized in Table 3.

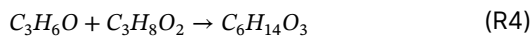
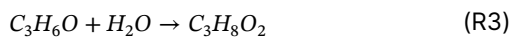


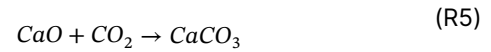
Table 3: Bioethanol production. Reactive dehydration parameters [11]

Reaction	Reaction R3	Reaction R4
Preexponential factor (s ⁻¹)	9.6x10 ⁷	75, 362
Activation energy (kJ/mol)	9.6x10 ⁶	82, 899

The solid fraction separated from the effluent is dried in DR-01. The generated vapor is condensed prior to being recycled to RD-01.

The dried solids are subsequently subjected to pyrolysis in reactor R-04, yielding bio-oil and biochar. These products are then routed to the gasification section (R-05), where they are converted into syngas. The produced syngas is upgraded via a Fischer-Tropsch (FT) synthesis in reactor R-06 [12], generating a broad hydrocarbon distribution ranging from C1 to C30. However, water and CO₂ are also formed as by-products. Therefore, the multiphase effluent from R-06 is sent to a flash tank (FT-02), which separates the stream into three phases. The aqueous phase is recovered as the third treated-water stream in the overall process. The hydrocarbon phase is directed to the biofuels refinement section, while the gas phase, mainly composed of CO₂, along with methane and hydrogen, is routed to the CO₂ capture section.

In the CaO-based capture configuration, the gas stream is fed to reactor R-07, where a selective carbonation reaction takes place. In this step, calcium oxide reacts with CO₂ to form calcium carbonate (CaCO₃), as described by reaction R5. The kinetic model employs an activation energy of 0.3699 kJ/mol and a pre-exponential factor of 10.2 s⁻¹ [13].



After CO₂ capture, the remaining gas stream, rich in methane and hydrogen, is recovered as a potential fuel product using cyclone CC-01. In parallel, the calcium carbonate particles are sent to reactor R-08, where calcination is performed to release the previously captured CO₂ and regenerate CaO. The resulting stream exiting R-08 is routed to a second cyclone (CC-02) to separate residual CO₂ from the regenerated solid. Finally, the recovered CaO is recycled back to reactor R-07.

The biofuels upgrading section consists of three distillation columns. Light gases are recovered as the overhead stream from DC-07, naphtha is obtained as the distillate from DC-08, and sustainable aviation fuel is recovered as the overhead stream from DC-09. The bottom product of DC-09 corresponds to green diesel.

Electrical power generation is achieved through an organic Rankine cycle (ORC) employing R245fa as the working fluid. The ORC recovers waste heat from different sections of the biorefinery through heat exchangers, including streams associated with DR-01, R-05, R-06, and RD-02.

In addition to the CaO-based configuration, a DES-based CO₂ capture alternative is assessed. The only difference between both biorefinery schemes lies in the CO₂ capture section. In the DES configuration, the gas mixture from FT-02 is fed to the bottom of an absorption column (AC-01), while a deep eutectic solvent (DES) is introduced from the top. The DES consists of choline chloride:urea and is used in a 1:1 DES:water ratio. The solvent selectively absorbs carbon-containing compounds, enabling hydrogen recovery as the overhead product, which is considered a valuable co-product.

The CO₂-loaded (exhausted) solvent stream (Ex-DES) is subsequently sent to flash tanks FL-03 and FL-04 for solvent regeneration and CO₂ release. The overhead stream from FL-04 corresponds to a residual gas containing approximately 80 mol% CO₂. The process flowsheet of the DES-based CO₂ capture configuration is presented in Figure 3.

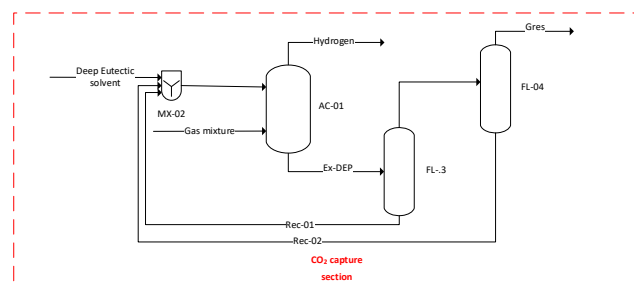


Figure 3. Process flowsheet for the DES-based CO₂ capture configuration.

The product slate obtained for each biorefinery configuration is summarized in Table 4. The reported water product corresponds to the total amount of treated water, obtained as the sum of all treated-water streams generated throughout the process. The resulting treated-water stream exhibits a COD of 19.1 ppm.

As shown in Table 4, the overall product yields are identical for both biorefinery configurations; the only differences are associated with the waste and hydrogen streams. In both the CaO-based and DES-based schemes, the waste stream is mainly composed of (i) the ethylene-formic acid stream generated in the ethanol/waste separation section, in addition to (ii) a residual gas stream and (iii) a CO₂-rich stream.

In both configurations, treated water is the dominant product, accounting for 70.5% of the total output. This is followed by sustainable aviation fuel, levulinic acid, naphtha, and light gases, contributing 4.13%, 2.20%, 2.10%, and 1.53%, respectively. The primary difference between the two schemes lies in the relative proportions of waste and hydrogen streams. In the CaO-based configuration, waste streams account for 17.21% of the total products, whereas in the DES-based configuration this fraction is reduced to 16.20%. As a result, hydrogen emerges as an additional valuable product in the DES-based scheme, representing 1.16% of the overall product distribution.

Table 4: Products obtained from the different schemes.

Product (kg/h)	CaO	DES
Scheme	Figure 2	Figure 3
Water	7,094.84	7,094.84
Levulinic acid	221.57	221.57
Light gases	153.62	153.62
Naphtha	211	211
Sustainable aviation fuel	415	415
Green diesel	74.8	74.8
Bioethanol	6.93	6.93
Di/Propylene glycol	49.3	49.3
Formic acid	96.4	96.4
Waste	1,730.26	1,631.49
Hydrogen	-----	117.01

The chemical oxygen demand (COD) removal capacity is defined as the relative reduction between the initial COD of the winery effluent and the final COD of the treated-water product. Based on this definition, the proposed biorefinery achieves a COD reduction of 99.99%, fully complying with the maximum COD limits established by Mexican regulations for water intended for human use (COD < 70 ppm), as specified in NOM-001-SEMARNAT-2021 and NOM-127-SSA1-2021. Nevertheless, even if the treated water were to reach excellent quality (e.g., COD ≈ 0 ppm), NOM-127-SSA1-2021 does not allow its direct use for drinking purposes. Instead, the treated-water

stream is suitable for internal reuse, such as recycled water within vineyard operations.

Regarding technical performance indicators, recovery is calculated exclusively for water and ethanol, as these are considered the relevant products of the biorefinery. Water recovery reaches 98.87% (Eq. (1)), based on the water content in the winery effluent as the input and the total treated water produced by the biorefinery as the output. In terms of sectional contributions, 84.73% of the recovered water is obtained from treated-water stream I, 13.56% from treated-water stream II, and the remaining fraction is generated within the Fischer-Tropsch section.

Ethanol recovery is relatively low (0.95%), as ethanol is produced solely as a bioethanol stream. It is important to emphasize that this outcome does not indicate an inefficient biorefinery configuration. Rather, it reflects the intentional process design, where ethanol contained in the winery effluent is primarily valorized as a feedstock for sustainable aviation fuel production pathway. Thus, only a small fraction of ethanol is available for recovery.

Table 5: Technical indicators

Technical parameter	CaO	DES
Scheme	Figure 2	Figure 3
Recuperation		
Water	98.87%	98.87%
Ethanol	0.95%	0.95%
Conversion		
Glucose	100%	100%
Solids	100%	100%
Ethanol	99.05%	99.05%
Calcium oxide	99.86%	-----
Yield		
Levulinic acid	65.19%	65.19%
Glycol	75.57%	75.57%
Ethylene	98.8%	98.8%
Calcium carbonate	99.99%	-----
Production mass ratio		
Light gases	0.0154	0.0154
Naphtha	0.0211	0.0211
Green diesel	0.0075	0.0075
Sustainable aviation fuel	0.0415	0.0415
Levulinic acid	0.0221	0.0221
Bioethanol	0.0007	0.0007
Water	0.7095	0.7095
Glycols	0.0049	0.0049
Formic acid	0.0088	0.0088
Wastes	0.173	0.1631

The product ratios reported in Table 5 provide valuable input for subsequent systems-level analyses, including supply chain development. These ratios can be directly incorporated into mathematical models to represent process outputs, thereby avoiding the introduction

of complex nonlinearities that typically arise when embedding detailed process simulations into optimization frameworks.

The main economic indicators of the proposed bio-refinery are summarized in Table 6. A comparative assessment of the economic indicators for the CaO- and DES-based configurations reveals a significant reduction of 48.86% in raw material costs when CaO is replaced by DES. This reduction is primarily attributed to the internal generation of hydrogen within the CO₂ capture section, which supplies the hydrogen required for alkene hydrogenation in the alcohol-to-jet pathway. Specifically, hydrogen is produced in unit AC-01. In contrast, in the CaO-based configuration, hydrogen must be purchased as a raw material, accounting for 50.16% of the total raw material cost. The DES-based scheme also exhibits a 2.45% increase in product sales relative to the CaO-based configuration. This improvement is mainly associated with hydrogen recovery as a valuable product. In the CaO scheme, hydrogen is effectively wasted due to the lack of purification capability. In the DES-based process, hydrogen becomes the third most abundant product, following levulinic acid and sustainable aviation fuel, contributing 91.22% and 3.39% of the product distribution, respectively.

Table 6: Economic indicators

	CaO	DES
Scheme	Figure 2	Figure 3
Raw material (USD/y)	\$1,138,265.10	\$582,134.16
Products (USD/y)	\$255,625,939.62	\$261,888,720.64
Utilities (USD/y)	\$21,848,553.72	\$21,901,820.16
Equipment cost (USD)	\$50,954,841.13	\$53,374,306.62
Annualized equipment cost (USD/y)	\$5,985,136.52	\$6,269,326.03
Total annual cost (USD/y)	\$28,971,887.65	\$28,753,280.34
Profit (USD/y)	\$226,654,024.68	\$233,135,440.3

Despite these advantages, utility and equipment costs increase by 0.24% and 4.75%, respectively, in the DES-based configuration compared to the CaO-based scheme. The higher equipment cost is mainly driven by the inclusion of a compressor required to feed CO₂ to unit AC-01 and a heat exchanger used to pretreat the DES prior to absorption, operating at 20 atm and 15 °C. In the DES-based scheme, the compressor and heat exchanger

represent 2.67% and 2.09% of the total equipment cost, respectively. By comparison, all equipment associated with CO₂ capture in the CaO-based scheme accounts for only 0.57% of the total equipment cost.

Regarding utility costs, the CO₂ capture section in the CaO-based configuration requires \$32.97 USD h⁻¹, while the DES-based configuration requires \$38.76 USD h⁻¹. These values correspond to 1.32% and 1.55% of the total utility costs of each process, respectively, explaining the observed 0.24% increase. In the CaO-based scheme, utility consumption is mainly associated with reactors R-07 and R-08, whereas in the DES-based scheme it includes the compressor feeding AC-01, the heat exchanger, and flash tanks FL-03 and FL-04.

Overall, the total annual cost is reduced by 0.75% in the DES-based configuration relative to the CaO-based scheme. As a result, the difference between revenues and operating costs leads to a 2.86% increase in profit for the DES-based process.

Table 7 summarizes the selected environmental indicators used for CO₂ quantification. In terms of CO₂-equivalent emissions associated with utilities, the DES-based scheme achieves a reduction of 0.48% compared to the CaO-based configuration. Although the CaO-based scheme releases a substantial amount of CO₂ due to CaCO₃ calcination during CaO regeneration, the DES-based scheme is unable to significantly reduce overall emissions. This limitation is mainly attributed to the large flowrate of exhausted DES (12.17 t h⁻¹) and the energy-intensive desorption step, which requires heating and handling a high mass of solvent, resulting in CO₂ emissions comparable to those of the CaO-based process.

Table 7: Environmental indicators

	CaO	DES
Scheme	Figure 2	Figure 3
CO ₂ e utilities (Ton CO ₂ /y)	431,843.59	429,766.75
CO ₂ streams (Ton CO ₂ /y)	12,015.37	11,894.15
Total	443,858.96	441,660.90

The CO₂ streams correspond to the desorption stages in which both CaO- and DES-based systems release the captured CO₂. The DES-based configuration exhibits a slightly lower CO₂ release, with a reduction of 1.01% compared to the CaO-based scheme. This behavior is attributed to partial CO₂ retention within the DES matrix, whereas in the CaO-based process CO₂ is almost entirely released during regeneration.

Although the relative difference in total CO₂ emissions between the CaO- and DES-based configurations is modest (approximately 0.5%), the absolute impact is significant. The DES-based process enables an annual reduction of 2,198 t CO₂, highlighting its environmental

relevance despite the small percentage difference.

CONCLUSIONS

This study demonstrates the technical and economic feasibility of producing value-added chemicals and biofuels from winery effluents through the modelling and simulation of an integrated biorefinery scheme. The proposed process enables the recovery of levulinic acid, propylene glycol, formic acid, and biofuels, including light gases, naphtha, sustainable aviation fuel, green diesel, and bioethanol, transforming an agro-industrial waste stream into a diversified portfolio of marketable products.

From a circular economy perspective, the proposed biorefinery closes material and energy loops by simultaneously valorizing organic matter, recovering water for internal reuse, and separating CO₂ emissions from hydrogen mixtures through the incorporation of deep eutectic solvents (DES) as a capture and utilization strategy. This approach reduces dependency on external raw materials, lowers total annual costs, and enhances profitability by integrating hydrogen as an additional value-added product. Moreover, the DES-based configuration contributes to emissions mitigation, reinforcing the environmental performance of the system while maintaining economic competitiveness. For the selected case study, in Baja California, Mexico, the biorefinery achieves attractive economic indicators and complies with national environmental and water quality regulations. In particular, a COD removal efficiency of 99.99% allows the recovery of treated water suitable for internal reuse, in accordance with NOM-001-SEMARNAT-2021 and NOM-127-SSA1-2021.

Overall, the proposed scheme exemplifies a circular and sustainable pathway for winery effluent management; this proposal allows shifting from waste treatment to resource recovery, and highlighting the role of integrated biorefineries as enabling technologies for the transition toward low-carbon and circular agro-industrial systems.

ACKNOWLEDGEMENTS

The authors acknowledge the support provided by Secretaría de Ciencia, Humanidades, Tecnología e Innovación (SECIHTI, México) for the financial support granted to develop the post-doctoral research (grant no. 2397403) of C. E. Guzmán-Martínez.

AUTHOR IDENTIFIERS

Author ORCIDs:

Guzmán-Martínez C.E: 0000-0002-3404-2650

Caltzontzin-Rabell V: 0000-0002-5739-0957

Martínez-Guido S.I: 0000-0002-0198-9338

Hernández S: 0000-0002-4598-3392

Gutiérrez-Antonio C: 0000-0002-7557-2471

REFERENCES

1. Mader AE, Holtman GA, Welz PJ. Treatment wetlands and phyto-technologies for remediation of winery effluent: challenges and opportunities. *Science of The Total Environment* 807:150544 (2022).
<https://doi.org/10.1016/j.scitotenv.2021.150544>
2. https://www.oiv.int/sites/default/files/documents/OIV_State_of_the_world_Vine_and_Wine_sector_in_2022_2.pdf (accessed February 25).
3. Buitrón G, Martínez-Valdez FJ, Ojeda F. Biogas production from a highly organic loaded winery effluent through a two-stage process. *Bioenerg. Res.* 12:714–721 (2019).
<https://doi.org/10.1007/s12155-019-09984-7>
4. Romero-García AG, Ramírez-Márquez C, Sánchez-Ramírez E, Ponce-Ortega JM, González-Campos JB, De Blasio C, Segovia-Hernández JG. Implementation of the deep eutectic solvent, choline urea chloride (1:2), to evaluate the sustainability of its application during CO₂ capture. *Process Integr Optim Sustain* 8:741–758 (2023).
<https://doi.org/10.1007/s41660-023-00383-2>
5. Felder, R. M., Rousseau, R. W., & Bullard, L. G. (2020). *Elementary principles of chemical processes*. John Wiley & Sons.
6. Turton, R., Bailie, R. C., Whiting, W. B., & Shaeiwitz, J. A. (2008). *Analysis, synthesis and design of chemical processes*. Pearson Education.
7. De Iseppi A, Lomolino G, Marangon M, Curioni A. Current and future strategies for wine yeast lees valorization. *Food Research International* 137:109352 (2020).
<https://doi.org/10.1016/j.foodres.2020.109352>
8. Carlson, E. C.: Don't Gamble with Physical Properties for Simulations. *Chemical Engineering Progress*, 35–46 (1996)
9. Romero-García AG, Ramírez-Corona N, Sánchez-Ramírez E, Alcocer-García H, De Blasio C, Segovia-Hernández JG. Sustainability assessment in the CO₂ capture process: multi-objective optimization. *Chemical Engineering and Processing - Process Intensification* 182:109207 (2022).
<https://doi.org/10.1016/j.cep.2022.109207>
10. Solis-Sanchez JL, Alcocer-Garcia H, Sanchez-Ramirez E, Segovia-Hernandez JG. Innovative reactive distillation process for levulinic acid production and purification. *Chemical Engineering Research and Design* 183:28-40 (2022).
<https://doi.org/10.1016/j.cherd.2022.04.041>
11. Guzmán-Martínez, C. E., Castro-Montoya, A. J., &

- Nápoles-Rivera, F. (2019). Economic and environmental comparison of bioethanol dehydration processes via simulation: reactive distillation, reactor–separator process and azeotropic distillation. *Clean Technologies and Environmental Policy*, 21, 2061-2071.
12. Guzmán-Martínez CE, Caltzontzin-Rabell V, Martínez-Guido SI, Gutiérrez-Antonio C. Valorization of effluents from the wine industry through a biorefinery scheme to obtain sustainable aviation fuel, levulinic acid, water, and value-added compounds. *Biochemical Engineering Journal* 221:109798 (2025).
<https://doi.org/10.1016/j.bej.2025.109798>
13. Kinoshita C. Production of hydrogen from bio-oil using cao as a CO2 sorbent. *International Journal of Hydrogen Energy* : (2003).
[https://doi.org/10.1016/s0360-3199\(02\)00203-3](https://doi.org/10.1016/s0360-3199(02)00203-3)

© 2026 by the authors. Licensed to PSEcommunity.org and PSE Press. This is an open access article under the creative commons CC-BY-SA licensing terms. Credit must be given to creator and adaptations must be shared under the same terms. See <https://creativecommons.org/licenses/by-sa/4.0/>

